

See discussions, stats, and author profiles for this publication at: <https://www.researchgate.net/publication/50286513>

# A Hypervalent Pentacoordinate Boron Compound with an N-B-N Three-Center Four-Electron Bond

ARTICLE *in* THE JOURNAL OF ORGANIC CHEMISTRY · MARCH 2011

Impact Factor: 4.72 · DOI: 10.1021/jo1024656 · Source: PubMed

---

CITATIONS

8

---

READS

37

3 AUTHORS, INCLUDING:



Satoshi Kojima

Hiroshima University

113 PUBLICATIONS 1,347 CITATIONS

SEE PROFILE

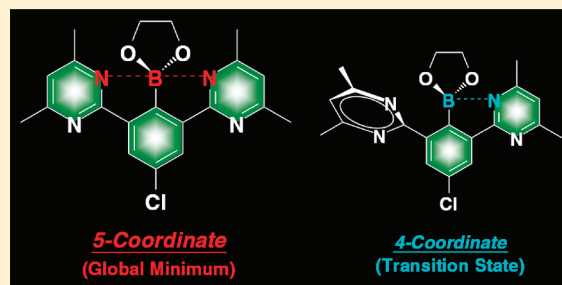
# A Hypervalent Pentacoordinate Boron Compound with an N–B–N Three-Center Four-Electron Bond

Yuichi Hirano, Satoshi Kojima, and Yohsuke Yamamoto\*

Department of Chemistry, Graduate School of Science, Hiroshima University, 1-3-1 Kagamiyama, Higashi-Hiroshima 739-8526, Japan

**S** Supporting Information

**ABSTRACT:** For the purpose of synthesizing and characterizing hypervalent boron compounds with strong hypervalent interaction, we have prepared a boron compound with a tridentate ligand bearing two pyrimidine rings as nitrogen donors. X-ray analysis and molecular orbital calculations suggested that the boron compound was of hypervalent pentacoordinate structure with an N–B–N hypervalent bond. Thus, we have prepared the first hypervalent second row element compound with apical N coordination. A breakdown of energy contributions by DFT calculations revealed that the N–B–N bond energy of the pentacoordinate state ground state (**13**) was 2.8 kcal mol<sup>−1</sup>. Implications were that the conjugation energy difference of 6.6 kcal mol<sup>−1</sup> (14.2–7.6 kcal mol<sup>−1</sup>) with the tetracoordinate state was a crucial factor for shifting stability toward the pentacoordinate structure.



## INTRODUCTION

Hypervalent compounds are main group element compounds in which the electron count of the central atom formally exceeds the number defined by the octet rule. Main group elements in and below the third row of the periodic table such as silicon, phosphorus, sulfur, and iodine are capable of expanding their valency to form such species, and many stable compounds with atoms bearing 10 formal electrons are known.<sup>1</sup> For second row elements such as carbon and boron, the corresponding electron state is found in the transition state of one of the fundamental organic reactions, the S<sub>N</sub>2 reaction, and the general conception is that these elements are reluctant to form stable hypervalent compounds. Although some theoretical calculations indicate the possibility of such compounds,<sup>2,3</sup> synthesis and isolation have posed an extremely difficult challenge.<sup>4</sup>

Recently, we developed a sterically rigid anthracene-type tridentate ligand and applied it as a scaffold for the synthesis of hypervalent carbon and boron compounds **1** and **2** (Figure 1).<sup>5</sup> Characterization by X-ray crystallographic analyses and density functional theory (DFT) calculations suggested that these compounds were hypervalent species. That is, the compounds were highly symmetric and the C–O and B–O distances were considerably shorter than the sum of the van der Waals radii.<sup>6</sup> Incidentally, the use of a similar rigid tridentate with two methoxy coordinating groups but with thioxanthene as the backbone was found useful for the synthesis of a compound that could be regarded as a hexacoordinate carbon compound.<sup>7</sup> However, the long C–O and B–O distances compared with corresponding general covalent bonds suggested that the attractive interactions were weak. Exchanging the aromatic carbon para

to the hypervalent boron in **2** to a more electron-withdrawing ammonium group (Me–N<sup>+</sup>) did not lead to a shortening of the B–O distance.<sup>8</sup> We attributed these results to the rigid nature of the tridentate ligand that limits bond shortening.

Since the capability to form short hypervalent bonds would require the apical donor groups to be attached to a more flexible backbone, carbon compounds **3** and boron compounds **4** using a van Koten-type tridentate ligand with oxygen donor sites were examined (Figure 1).<sup>9</sup> X-ray electron-density analyses and DFT calculations suggested that these compounds (**3** and **4**) were also hypervalent compounds. However, the C–O and B–O distances of the van Koten-type compounds **3** and **4** were longer than those of the anthracene-type compounds **1** and **2**, contrary to our expectations. For this ligand system it was found that pinacol derivative **4a** assumed tricoordinate structure, although the difference in the electronic nature of the boron atom compared with **4b** could be considered to be rather small (Figure 2). As another flexible tridentate system, 2,6-bis-(alkoxycarbonyl)-1-borylbenzenes were also examined.<sup>10</sup> The pinacol and catechol systems (**5a** and **5b**, respectively) were found to give pentacoordinate compounds with average B–O bond lengths shorter than those of the van Koten ligand system, but longer than those for the anthracene system. For this system, the diarylboryl-substituted compound **5c** was of the tetracoordinate state in which only one of the two oxygen atoms interacts with the central atom. These results show that for the flexible tridentate system, when the electrophilicity of the boron atom is weak or the nucleophilicity of the donor group is weak, the

**Received:** December 16, 2010

**Published:** March 04, 2011

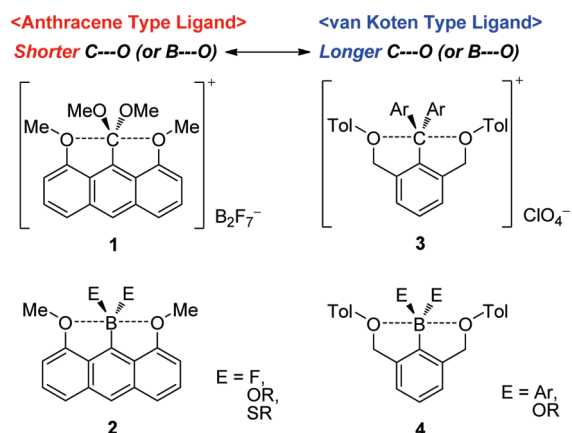
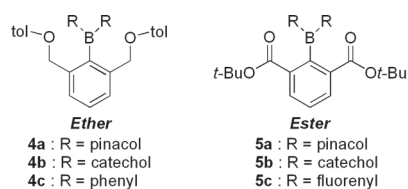


**Figure 1.** Pentacoordinate carbon and boron compounds of two ligand systems.



Substituents		Donicity Strength of the Oxygen Atoms	
		Ether	Ester
Electrophilicity of the Boron Atom	Pinacol	3.024(3), 3.155(3)	2.524(2), 2.570(2)
		<b>4a</b> : Tricoordinate	<b>5a</b> : <b>Pentacoordinate</b>
	Catechol	2.528(9), 2.660(9)	2.458(2), 2.560(2)
		2.496(9), 2.703(10)	<b>5b</b> : <b>Pentacoordinate</b>
	Diaryl	2.561(3), 2.749(4)	1.638(5), 3.110(5)
		2.539(3), 2.752(4)	<b>5c</b> : <b>Tetracoordinate</b>
		<b>4c</b> : <b>Pentacoordinate</b>	

**Figure 2.** Comparison of structures among boron compounds bearing different substituents.

compound tends to be tricoordinate, and when the strength of the two factors is intermediate, the compound becomes pentacoordinate. Furthermore, when both the electrophilicity of the boron atom and the nucleophilicity of the donor group are strong, the coordination state tends to be tetracoordinate.

To raise the strength of the interaction between the central atom and two donor atoms, other donor groups with higher coordination ability were also examined. For boron, compounds bearing two dialkylphosphino,<sup>11a</sup> dialkylamino,<sup>11b,12</sup> or alkylthio groups,<sup>5,13</sup> and for carbon, compounds bearing aryloxides<sup>11c,d</sup> were found to form unsymmetric tetracoordinate structures according to X-ray analyses. Thus, all in all, for strong donors, it seems that there is a preference for the formation of one strong bond over two weak bonds as in the case of **5c**. These results implied that groups with donor ability that is intermediate in strength between the weak alkoxy group and the strong alkylamino or alkylthio group were required. Aromatic nitrogen compounds seemed to be appropriate for this purpose as previously applied for other systems.<sup>15,16</sup> Since a symmetric system seemed adequate for our purpose, which included determination of the rotation barrier, we decided to introduce pyrimidine rings. Another advantage of this system that we envisaged was that the pentacoordinate state would have two effective aryl–aryl  $\pi$ -conjugations between the pyrimidine rings

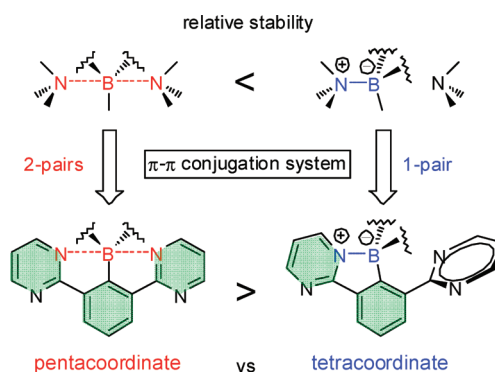
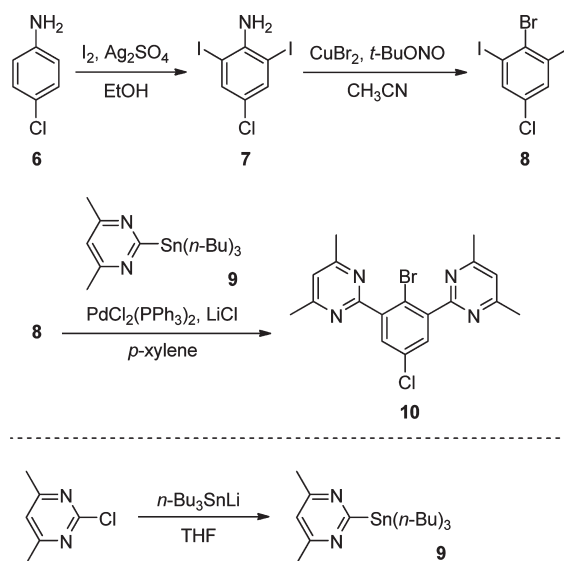


**Figure 3.** Working hypothesis for the pyrimidine ligand system.

### Scheme 1. Synthesis of the Tridentate Ligand Precursor Bearing Two Dimethylpyrimidine Rings



and the benzene ring while the tetracoordinate state would have just one. Thus, the former would have larger conjugation energy gain that might overcome the differences in bond energies between the weaker hypervalent bond in the former and the stronger single coordination bond in the latter (Figure 3).

Herein, we report on the synthesis, isolation, and characterization of a hypervalent pentacoordinate boron compound with an N–B–N three-center four-electron bond designed according to our working hypothesis. We also describe our estimation of the N–B–N bond strength along with analysis of energy contributions of the penta- and the tetracoordinate states based upon theoretical calculations.

## RESULT AND DISCUSSION

**Synthesis of the Tridentate Ligand Precursor and Incorporation of the Boron Moiety.** The precursor of the new tridentate ligand with two dimethylpyrimidine rings was prepared as described in Scheme 1. The underlining strategy for the target compound was that the chlorine atom was expected to improve crystallization and that the methyl groups of the pyrimidine rings were expected to both increase reactivity for

Scheme 2. Synthesis of Boron Compound 11 Bearing the Tridentate Ligand

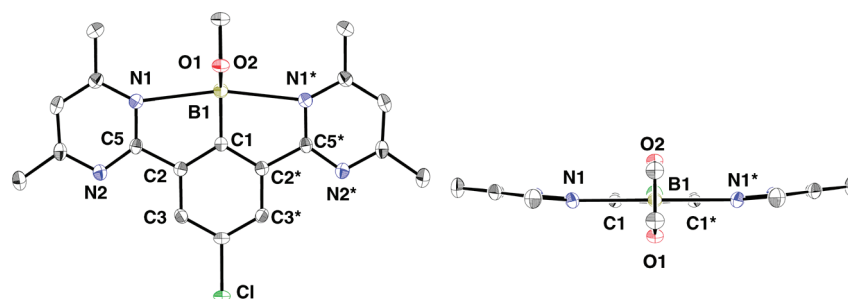
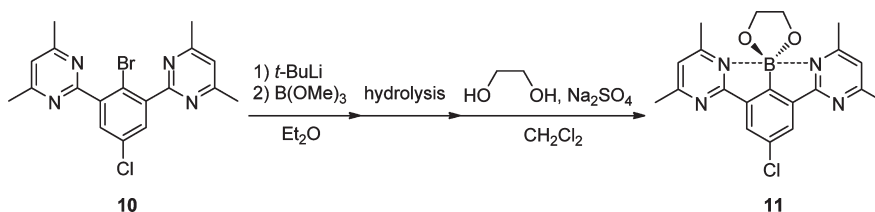


Figure 4. ORTEP drawing of 11 with thermal ellipsoids at the 50% probability level. All hydrogen atoms have been omitted for clarity.

Table 1. Selected Structural Parameters of the Structures Determined by X-ray Structural Analysis and Calculations (B3PW91/6-31G(d))

	X-ray (11)	calculation (12)	calculation (13)
bond distance/Å			
B1–N1	2.5371(12)	2.5918	2.6034
B1–N1*	2.5371(12)	2.5918	2.6034
bond angle/deg			
N1–B1–N1*	166.38(11)	165.39	164.78
C1–B1–N1	83.19(8)	82.70	82.24
C1–B1–N1*	83.19(8)	82.70	82.24
O1–B1–N1	93.93(5)	93.97	91.80
O1–B1–N1*	93.93(5)	93.97	91.80
dihedral angle/deg			
C3–C2–C5–N2	1.73(18)	0.00	12.55
C3–C2*–C5*–N2*	1.73(18)	0.00	12.55

the Stille coupling reaction and inhibit nucleophilic attack to the ring upon attempted incorporation of the boryl moiety. 4-Chloroaniline **6** was treated with  $I_2$  to give **7** in 69% yield.<sup>16</sup> Bromination of **7** by treatment with  $CuBr_2$  and  $t$ -BuONO afforded **8** in 68% yield.<sup>17</sup> The Stille coupling reaction of diiodide **8** with tin derivative **9** proceeded to yield **10** in 13% yield.<sup>18</sup> Thus, the precursor **10** was prepared from 4-chloroaniline **6** in 6% total yield. The low yield of the final step may have been caused by both the reactivity of the reagents, which was still insufficient, and the thermal instability of the product in solution at high temperature.

The introduction of the boryl moiety was attempted by lithiation of **10** followed by treatment with some boron compounds. However, this was found to be nontrivial and the diarylboryl group, for instance, could not be incorporated due to what we suspect to be steric repulsion by the methyl groups. Fortunately, the rather small methoxy borate reacted to give the dimethoxyboryl derivative. However, this was found to be extremely

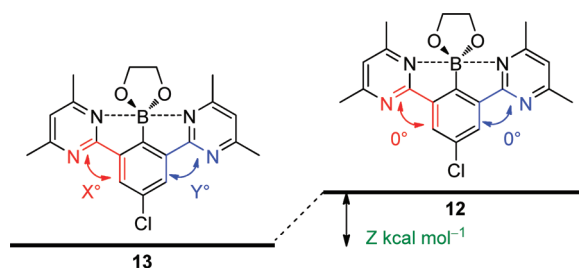
susceptible to moisture. Thus, the methoxy groups were exchanged with ethylene glycol to afford a 1,3,2-dioxaborolane derivative **11** (Scheme 2). This product was still sensitive to moisture but single crystals could be obtained.

**Structure of the Boron Compound Bearing the Tridentate Ligand.** Single crystals suitable for X-ray structural analysis were obtained as yellow plate crystals from a mixture of dry  $CH_2Cl_2$  and  $n$ -hexane under a  $N_2$  atmosphere. The X-ray structure of **11** is shown in Figure 4, and selected structural parameters are summarized in the left-hand column of Table 1.

The crystal structure of **11** shows the 1,3,2-dioxaborolane ring to be planar indicating that the boron atom is  $sp^2$  hybridized and this plane to be perpendicular to the phenyl group to which it is attached. Furthermore, the compound was completely symmetrical with respect to the plane of the central boryl ring. The central boron atom and two nitrogen atoms of the pyrimidine rings [N1–B1–N1\*: 166.38(11)°] were nearly colinear. In this geometry of the three atoms, the nitrogen atoms are oriented so that it is possible for the lone pair of each nitrogen atom to directly face the empty p-orbital of the central boron atom. Furthermore, the two B–N distances [B1–N1, B1–N1\*: 2.5371(12) Å] were substantially shorter than the sum of van der Waals radii (3.62 Å). These results suggest that the compound assumes trigonal bipyramidal (TBP) structure about the central boron atom (B1) with O1, O2, and C2 as the three equatorial atoms, and with two nitrogen atoms (N1 and N1\*) and the boron atom constituting an N–B–N three-center four-electron bond. The dihedral angles between the central benzene ring and the two pyrimidine rings [C3–C2–C5–N2, C3\*–C2\*–C5\*–N2\*: 1.73°] were near 0°, indicating there is maximum conjugative interaction among the three rings. The directions of the minute deviations were counterclockwise with respect to each other in a  $C_s$ -symmetry fashion, thereby creating a slight curvature of the backbone consisting of the three essentially coplanar rings.

**Insights on the N–B–N Bond of the Boron Compound.** To gain more insight on the N–B–N bond, the structure of **11** was optimized by ab initio molecular orbital calculations at the

Table 2. Comparison of Structural Parameters between Transition State 12 and Global Minimum 13



	HF/6-31G(d)	B3PW91/6-31G(d)	B3LYP/6-31G(d)	B3PW91/6-311++G(df,dp)	B3LYP/6-311++G(df,dp)
X	20	12.55	11.79	17.19	17.56
Y	20	12.55	11.79	17.19	17.56
Z	0.50	0.18	0.13	0.46	0.49

HF/6-31G(d) level and by hybrid density functional theory (DFT) calculations at several levels of calculation using the Gaussian 09 program,<sup>19</sup> with results shown in Table 2.

Optimization using the X-ray structure as the initial structure with the MO method gave conformer **12** (HF/6-31G(d)) with dihedral angles of 0° between the phenyl group and each pyrimidine ring as a transition state structure with a single negative frequency value. Further optimization in the direction of the negative vibration of **12** (HF/6-31G(d)) yielded conformer **13** (HF/6-31G(d)) with dihedral angles of 20° as the global minimum. In addition to the large deviation of the dihedral angle from the X-ray structure, the array of pyrimidine nitrogens and the central boron was not appropriate for assuming hypervalent interaction and in this case the boron atom is better described as a tricoordinate species. Thus, this MO method was not sufficient for reproducing the experimental results. For the hybrid methods, the B3PW91 and B3LYP functionals were used in combinations with basis sets of 6-31G(d) and 6-311++G(df,dp) for optimization. Similar to the MO calculations, the conformer with the two dihedral angles of 0° was found to be a transition state for all four calculations. As for the global minimum, the dihedral angles and the energy differences with conformer **12** were basis set dependent. The dihedral angle values were ca. 12° and 17° with the 6-31G(d) and 6-311++G(df,dp) basis sets, respectively, and the corresponding energy differences were ca. 0.15 and 0.48 kcal mol<sup>-1</sup>. Since the former smaller basis set seemed to be sufficient for obtaining structural parameters similar to those for the X-ray structure, we decided to use it for further computations. Furthermore, the B3PW91 functional has been found to be more superior to the B3LYP functional for reproducing structural parameters of X-ray structures for analogous hypervalent carbon and boron compounds bearing neutral oxygen donors at the apical positions with only a slight overestimation of the bond lengths (deviation: 0.1% to 1.2%).<sup>5,7–10</sup> Thus, this functional was adopted in a combination with the 6-31G(d) basis set. Selected structural parameters of the two states deduced with the B3PW91/6-31G(d) method are shown in Table 1 alongside the experimental data. The geometry of **12**, a transition state, was C<sub>2v</sub> symmetrical with two identical B–N bond lengths (2.5918 Å), which were slightly longer (2.2%) than the experimental data (2.5371(12) Å), and the dihedral angles between the central benzene ring and each pyrimidine ring were 0.00°, which is smaller than the experimental value of

1.73°. Otherwise, the structure of the conformer was practically the same as the X-ray structure. As for the global minimum, the dihedral angles were both 12.55° in a conrotatory manner. The dioxaborolane plane was also rotated in the same direction in a gear-like sense, all together making the conformer pseudo-C<sub>2</sub> symmetric in contrast to the C<sub>s</sub>-type structure of **11**, deviations of which were actually negligible. Disregarding these features, conformer **13** had structural parameters very similar to those of **12**, as shown in Table 1. The reason for the twisting seems to be the small but not negligible steric hindrance between the dioxaborolane plane and the methyl groups of the pyrimidine rings flanking this plane. A point to note is that the energy difference between “transition state” **12** and global minimum **13** was found to be only 0.18 kcal mol<sup>-1</sup>, indicating that the energy potential surface in the vicinity of the minimum is rather flat. Thus, it is not unreasonable to assume that the discrepancy in geometry between experiment and theory is brought about by crystal lattice forces that cancel out the steric hindrance.

The molecular orbitals (MOs) of **12**, which is structurally close to the X-ray structure but is a “transition state”, add support for the presence of a three-center four-electron bond (Figure 5). HOMO–16, HOMO–11, and LUMO+12 can be regarded as the bonding, nonbonding, and antibonding orbitals of the three-center four-electron bond, respectively. HOMO–16, in particular, is suggestive of attractive interaction by donation of lone pair electrons from one nitrogen atom of each pyrimidine into the vacant p orbital on the central boron atom. The corresponding orbitals of **13**, the global minimum, have energy levels that are the same as those for **12**. Furthermore, the appearances are essentially the same as those of **12**, in spite of lower symmetry, with the only differences visually showing in LUMO+12, the antibonding orbital. Especially noteworthy is that although the dihedral angle is deviated away (12°) from the ideal angle of 0° as in **12**, the bonding orbitals of **13** are still suggestive of similar attractive interactions. Thus, small structural deviations do not seem to change electronic features. Natural bond orbital (NBO) analysis indicated that the N–B–N hypervalent bond energy of **13** was 2.4 kcal mol<sup>-1</sup>.

**Elucidation of the Tetracoordinate Rotational Transition State.** We have previously used the variable-temperature NMR coalescence method for measuring the rotation barrier of similar pyrimidine rings in compounds bearing the N–S–N bond for evaluating hypervalent interaction in these sulfur compounds,<sup>14</sup> and the method seemed suitable for determining the rotation



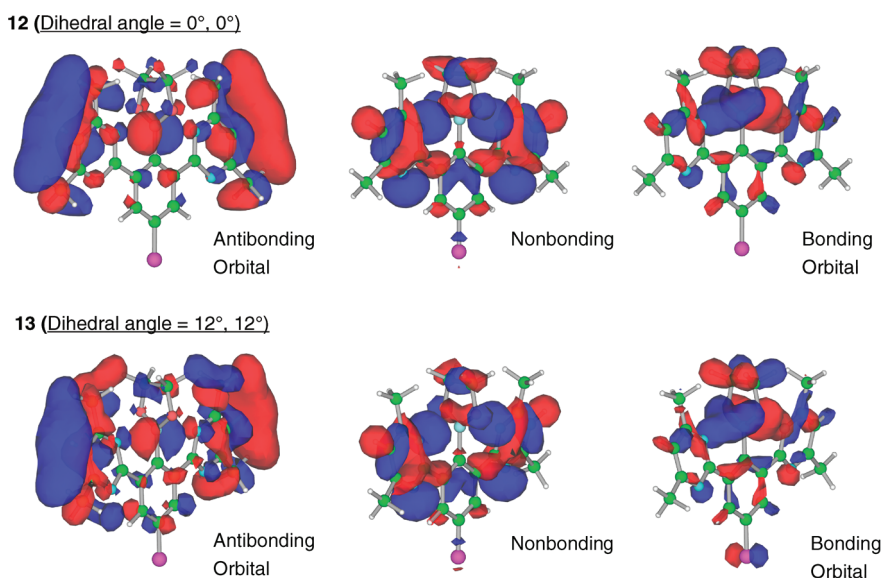


**Figure 5.** Molecular orbitals of **12** and **13** (threshold:  $2.1 \times 10^{-4} \text{ eV}^{-3/2}$  for the bonding orbital,  $1.4 \times 10^{-4} \text{ eV}^{-3/2}$  for the others): antibonding orbital (left), LUMO+12 (3.0 eV); nonbonding orbital (center), HOMO−11 (−8.4 eV); bonding orbital (right), HOMO−16 (−9.3 eV), respectively, for both sets of orbitals.

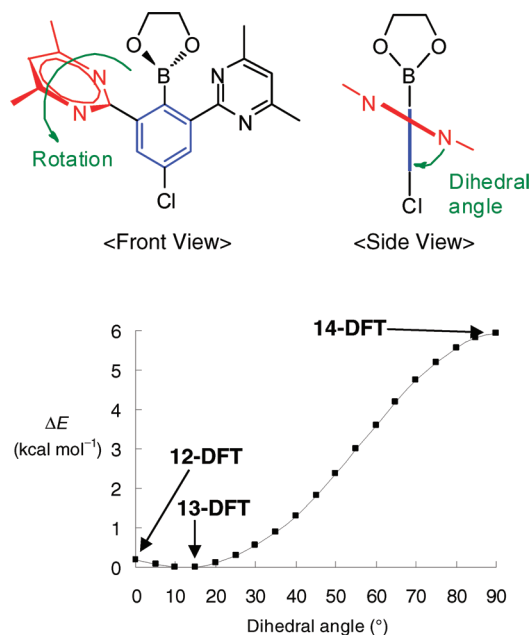


**Figure 6.** Energy diagram for **11** with restricted rotation of the pyrimidine ring, calculated at the B3PW91/6-31G(d) level.

barrier for compound **11**. However, presumably due to the low energy barrier for stereomutation, no separation of the pyrimidine methyl signals, which are inequivalent in a frozen state, could be observed even at low temperatures with a 600 MHz NMR instrument. Thus, we resorted to theoretical calculations. To get a schematic view of the rotation process, the dihedral angle between the central benzene ring and one of the side pyrimidine rings was varied from 0° to 90° with increments of 5° and the structures were optimized at each degree by using theoretical calculations at the B3PW91/6-31G(d) level. The results are shown in Figure 6. The figure shows a near sigmoidal curve, indicating that the rotation is rather straightforward with no apparent complications.

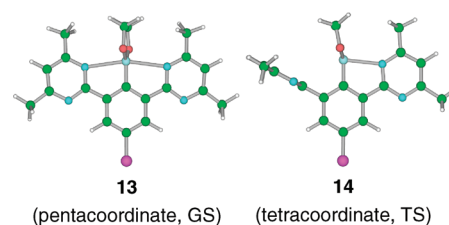


**Figure 7.** Optimized structures of **13** (pentacoordinate, GS) and **14** (tetracoordinate, TS). Dihedral angles between the central benzene and each pyrimidine ring are 12°, 12° for **13** and 90°, 0° for **14**. Transition state **14** is 6.0 kcal mol<sup>−1</sup> higher in energy than **13**.

The local maximum **14** had dihedral angles of 90° and 0°, as would be expected. The calculated structure of **14** along with that of **13** is shown in Figure 7.

Conformer **14** with the dihedral angles of 90° and 0° was found to be a transition state structure with only one negative frequency of  $-34.8 \text{ cm}^{-1}$  with vibration vectors which coincide with the direction of the rotation of the pyrimidine ring with respect to the pyrimidine–benzene bond. Contrary to expectations, the degree of pyramidalization of the boron atom is small and its appearance is closer to the tricoordinate state rather than the tetracoordinate state. However, the orientation of the pyramidalization is one in which the larger lobe of the vacant orbital of the boron atom faces the pyrimidine nitrogen. This implies that there is B–N interaction, although it may be weak. Natural bond orbital (NBO) analysis indicated that the B–N bond energy of **14** was 14.1 kcal mol<sup>−1</sup>, which is rather small but much larger than that for the N–B–N bond (2.4 kcal mol<sup>−1</sup>) in **13**. The difference in energy between **13** and **14**, which corresponds to the rotation barrier of one of the pyrimidine rings, was calculated as 6.0 kcal mol<sup>−1</sup>. This low value is reasonable considering the fact that the rotation barrier could not be experimentally determined. There is also the possibility of a tricoordinate boron conformer in which the dioxaborolane plane is in conjugation with the phenyl ring as the transition state for the rotation, though additional motions such as scission of the other

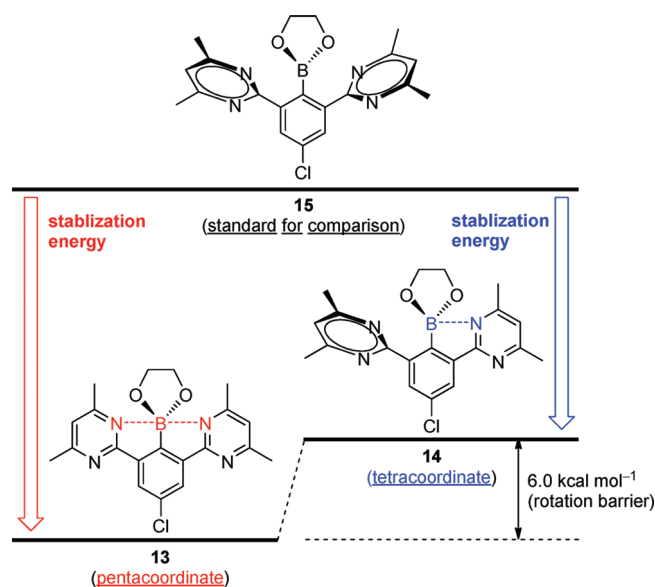


Figure 8. Comparison of stabilization energy.

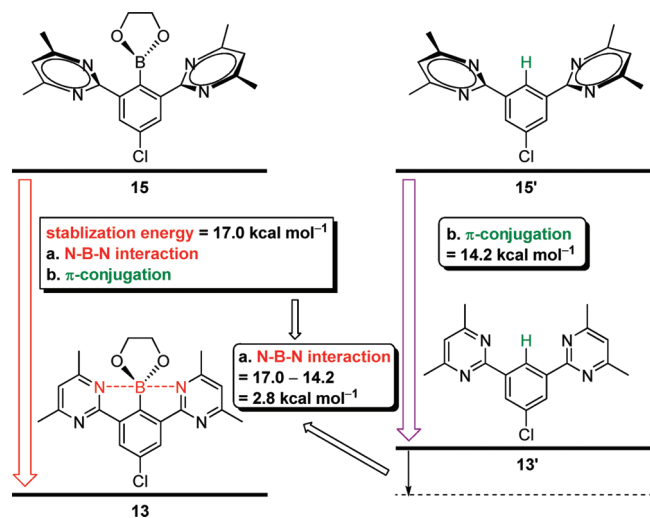


Figure 9. Determination of stabilization energy in the pentacoordinate structure.

B–N bond and B–C (phenyl) bond rotation are additionally required. However, it was found by computational optimizations that such a conformer would be less stable than 13 by 11.4 kcal mol<sup>-1</sup> and 14 by 5.4 kcal mol<sup>-1</sup>, respectively. In this conformer, the pyrimidine–benzene dihedral angles were both 45° and the dioxaborolane–benzene dihedral angle was 20°. Therefore, this conformer can be excluded as a relevant state.

**Estimation of the Energy Relationship between the Pentacoordinate and Tetracoordinate States.** A major factor contributing to the stabilization of conformer 13 other than N–B–N interaction is conjugation energy gained upon coplanarization of the pyrimidine rings and the benzene ring.<sup>20</sup> Thus, the approximation of the conjugation energy would be important to elucidate the reason why the pentacoordinate state was more stable than the tetracoordinate state. To this end, we assumed conformer 15, in which the dioxaborolane plane is fixed with the same geometry as 13 and the two pyrimidine rings are oriented perpendicular to the phenyl ring. This conformer is expected to

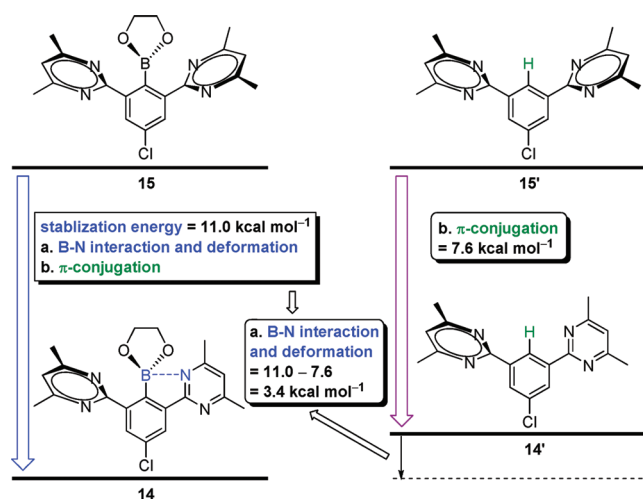


Figure 10. Determination of stabilization energy in the tetracoordinate structure.

have minimum N–B–N interaction and conjugation energy. Thus, the energy difference between stable state 13 and 15 should correspond to the sum of N–B–N interaction and conjugation energy. A one-point calculation at the B3PW91/6-31G(d) level for 15 gave the value of 17.0 kcal mol<sup>-1</sup> for the energy difference with 13 (Figure 8).

To estimate the contribution of just the conjugation energy by the two pyrimidine–benzene coplanarizations, we have also calculated the energy difference between species 13' and 15' which have the boryl moiety replaced by a hydrogen atom in 13 and 15 with other geometric features kept the same, respectively (Figure 9). The difference was computed to be 14.2 kcal mol<sup>-1</sup>, thereby suggesting that the sum of the stabilization gain by conjugation is 14.2 kcal mol<sup>-1</sup> (7.1 kcal mol<sup>-1</sup> per one coplanarization), and N–B–N interaction which corresponds to the difference is 2.8 kcal mol<sup>-1</sup> (17.0–14.2 kcal mol<sup>-1</sup>). This value is in good agreement with the value of 2.4 kcal mol<sup>-1</sup> from the NBO analysis.

In the case of the tetracoordinate 14, upon transformation from 15, in addition to the gain of energy from one coplanarization and the formation of the B–N coordination bond, loss of energy due to weakening of the other three bonds involving the boron atom could be perceived as a major contribution to the overall energy (Figure 10). Thus, the sum of these energies could be regarded as 11.0 kcal mol<sup>-1</sup> (Figure 8). Exchanging the boryl group with a hydrogen atom in 14 to 14' and carrying out a one-point calculation gave 7.6 kcal mol<sup>-1</sup> as the difference in energy. This would correspond to the conjugation energy, and the fact that the conjugation energy of 13' was estimated to be essentially 2-fold of that of 14' implies that our approximations are justified. The difference of 3.4 kcal mol<sup>-1</sup> (11.0–7.6 kcal mol<sup>-1</sup>) can be regarded as the sum of B–N bond energy gain and energy loss upon deformation of the geometry of the boron atom.

The overall results are summarized in Figure 11. Implications are that the energy of the N–B–N bond in the pentacoordinate structure (2.8 kcal mol<sup>-1</sup> by derivation or 2.4 kcal mol<sup>-1</sup> by NBO analysis) is weaker than that of a single B–N bond in the tetracoordinate structure (14.1 kcal mol<sup>-1</sup> by NBO analysis). By itself this would mean that the formation of the hypervalent N–B–N is unfavorable compared with tetracoordination by a single B–N. However, owing to the large energy gain by π-conjugation stabilization upon assuming pentacoordinate structure (14.2 kcal

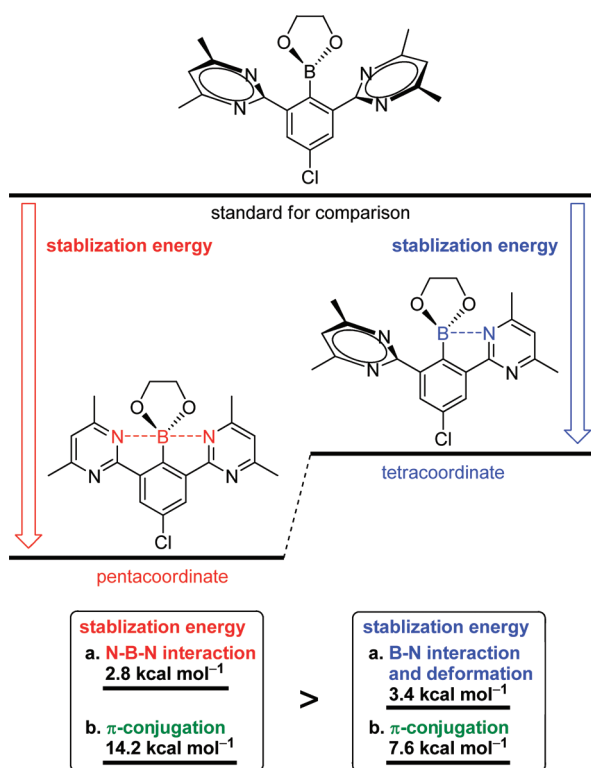


**Figure 11.** Comparison of stabilization energy between the pentacoordinate and the tetracoordinate species.

$\text{mol}^{-1}$ ) compared with that for the tetracoordinate structure ( $7.6 \text{ kcal mol}^{-1}$ ) combined with deformation energy loss, the total stabilization energy in the pentacoordinate structure has become larger than that for the tetracoordinate structure, thereby making the pentacoordinate structure more favorable.

## CONCLUSION

To gain further knowledge of hypervalent compounds of second row elements, we have synthesized a new tridentate bearing two pyrimidine rings, and have utilized it for the synthesis, isolation, and characterization of the first hypervalent pentacoordinate boron compound with an N–B–N three-center four-electron bond, which also happens to be the first of its kind for all second row elements. This was achieved although the coordinating sites were less geometrically constricted than the anthracene backbone system. In this structure, the two pyrimidine rings and the central benzene ring were found to be essentially coplanar, whereas theoretical calculations at the B3PW91/6-31G(d) level predicted a slightly distorted ground state with pyrimidine–benzene dihedral angles of  $12.55^\circ$ . However, the potential surface within this angle range was shallow with an energy difference between optimized structures with dihedral angles of  $0^\circ$  and  $12.55^\circ$  being only  $0.18 \text{ kcal mol}^{-1}$ . This suggested, at least for our system, that small deviations in the structure do not divert the electronic property of the species. By breaking down the energies of stabilization of the stable pentacoordinate conformer into conjugation energy and bond energy of the N–B–N, and combining calculations, we could estimate the N–B–N bond energy to be  $2.8 \text{ kcal mol}^{-1}$ . Although the approximation was made by indirect means, it was in good agreement with the value of  $2.4 \text{ kcal mol}^{-1}$  derived from NBO analysis, and thus the elucidated value should give an indication of the

magnitude of such bonds. The large difference in conjugation energy between the pentacoordinate and tetracoordinate states indicated that the utilization of conjugation energy gain is an effective strategy for obtaining hypervalent species in favor of prospectively stable tetracoordinate species. Attempts to experimentally determine the hypervalent bond strength and to utilize our findings in preparing analogues with other nitrogen heterocycles are in progress.

## EXPERIMENTAL SECTION

**General Procedures.** The  $^1\text{H}$  NMR (400 MHz) chemical shifts ( $\delta$ ) are given in ppm downfield from  $\text{Me}_4\text{Si}$ , determined by residual  $\text{CHCl}_3$  ( $\delta = 7.26 \text{ ppm}$ ) or  $\text{CDHCl}_2$  ( $\delta = 5.30 \text{ ppm}$ ). The  $^{11}\text{B}$  NMR (127 MHz) chemical shifts ( $\delta$ ) are given in ppm downfield from the external  $\text{BF}_3 \cdot \text{Et}_2\text{O}$  ( $\delta = 0 \text{ ppm}$ ). The  $^{13}\text{C}$  NMR (100 MHz) chemical shifts ( $\delta$ ) are given in ppm downfield from  $\text{Me}_4\text{Si}$ , determined by  $\text{CDCl}_3$  ( $\delta = 77.0 \text{ ppm}$ ). The  $^{119}\text{Sn}$  NMR (149 MHz) chemical shifts ( $\delta$ ) are given in ppm downfield from the external  $\text{Me}_4\text{Sn}$  ( $\delta = 0 \text{ ppm}$ ).

THF,  $\text{Et}_2\text{O}$ , and *n*-hexane were purified by passing through a Glass Contour solvent dispensing system under  $\text{N}_2$  atmosphere.  $\text{CH}_2\text{Cl}_2$  and  $\text{CH}_3\text{CN}$  were purified by distilling from  $\text{CaH}_2$  under a  $\text{N}_2$  atmosphere. Column chromatography was carried out by using silica gel or reverse-phase HPLC. 2-Chloro-4,6-dimethylpyrimidine was synthesized according to a literature procedure.<sup>21</sup>

**Synthesis of 4-Chloro-2,6-diiodoaniline (7).** To a solution of  $\text{I}_2$  (2.84 g, 11.2 mmol) in  $\text{EtOH}$  (40 mL) was added  $\text{Ag}_2\text{SO}_4$  (3.49 g, 11.2 mmol) followed by 4-chloroaniline (6) (510 mg, 4.00 mmol) at room temperature. After being stirred for 1 h at room temperature, the suspension was concentrated by using a rotary evaporator and the residue was dissolved in  $\text{AcOEt}$  (150 mL). The organic layer was washed with sat.  $\text{Na}_2\text{S}_2\text{O}_3$  aq ( $2 \times 100 \text{ mL}$ ) and dried over  $\text{Na}_2\text{SO}_4$ . The solvent was removed by using a rotary evaporator. Compound 7 (1.04 g, 2.75 mmol, 69%) was obtained as a black solid.  $^1\text{H}$  NMR ( $\text{CDCl}_3$ ,  $\delta$ ) 7.62 (s, 2H), 4.61 (br s, 2H). Mp  $128.9\text{--}129.7^\circ\text{C}$  (lit.<sup>22</sup> mp  $129^\circ\text{C}$ ).

**Synthesis of 1-Bromo-4-chloro-2,6-diiodobenzene (8).** To a solution of 7 (1.04 g, 2.75 mmol) in dry  $\text{CH}_3\text{CN}$  (50 mL) was added  $\text{CuBr}_2$  (3.07 g, 13.8 mmol) followed by *t*-BuONO (0.52 mL, 4.1 mmol) at room temperature. After being stirred for 12 h at  $50^\circ\text{C}$ , the reaction mixture was cooled to room temperature and treated with sat.  $\text{NaHCO}_3$  aq (50 mL). The reaction mixture was extracted with  $\text{AcOEt}$  ( $3 \times 50 \text{ mL}$ ). The combined organic layer was washed with sat.  $\text{Na}_2\text{S}_2\text{O}_3$  aq (100 mL) and dried over  $\text{Na}_2\text{SO}_4$ . The solvent was removed by using a rotary evaporator. The crude product was purified by silica gel column chromatography ( $\text{CH}_2\text{Cl}_2$ ,  $R_f$  0.90). Compound 8 (830 mg, 1.87 mmol, 68%) was obtained as a black solid. Colorless single crystals suitable for X-ray structural analysis were obtained by recrystallization from  $\text{EtOH}$  in the open air.  $^1\text{H}$  NMR ( $\text{CDCl}_3$ ,  $\delta$ ) 7.84 (s, 2H).  $^{13}\text{C}$  NMR ( $\text{CDCl}_3$ ,  $\delta$ ) 139.5 (CH), 134.6 (C), 133.8 (C), 99.6 (C). HRMS (APPI, positive) calcd ( $m/z$ ) for  $[\text{C}_6\text{H}_2\text{BrClI}_2]^+ \cdot 441.71124$ , found 441.71124. Elemental analysis calcd (%) for  $\text{C}_6\text{H}_2\text{BrClI}_2$  with  $0.5\text{C}_2\text{H}_6\text{O}$  (residual solvent from crystallization): C 17.73, H 1.06. Found: C 17.57, H 1.02. Mp  $123.6\text{--}124.4^\circ\text{C}$ .

**Synthesis of 4,6-Dimethyl-2-(tri-*n*-butylstannyl)pyrimidine (9).** To a solution of (*i*-Pr) $_2\text{NH}$  (8.40 mL, 68.0 mmol) in dry THF (70 mL) was added dropwise *n*-BuLi (1.58 M in *n*-hexane, 38.6 mL, 61.0 mmol) at  $0^\circ\text{C}$ . After 30 min of stirring, (*n*-Bu) $_3\text{SnH}$  (15.5 mL, 57.0 mmol) was added dropwise to the solution. After being stirred for 10 min, the mixture was cooled to  $-78^\circ\text{C}$ . The solution was slowly transferred with vigorous stirring to a solution of 2-chloro-4,6-dimethylpyrimidine (7.65 g, 54.0 mmol) in dry THF (70 mL) at  $-78^\circ\text{C}$ . After being stirred for 2 h, the solution was allowed to warm to  $0^\circ\text{C}$ . After 2 h of stirring, the reaction mixture was quenched with  $\text{H}_2\text{O}$  (50 mL). The reaction mixture was extracted with  $\text{AcOEt}$  ( $3 \times 200 \text{ mL}$ ). The combined organic layer was washed with brine (400 mL) and dried



over Na<sub>2</sub>SO<sub>4</sub>. The solution was filtered through a pad of silica gel and the silica gel was washed with AcOEt (400 mL). The filtrate was concentrated by using a rotary evaporator. The crude product was purified by silica gel column chromatography (AcOEt: *n*-hexane = 1:10, *R<sub>f</sub>* 0.25). Compound **9** (13.6 g, 46.8 mmol, 87%) was obtained as a colorless oil. <sup>1</sup>H NMR (CDCl<sub>3</sub>, δ) 6.82 (s, 1H), 2.41 (s, 6H), 1.58 (quint, <sup>3</sup>*J* = 8 Hz, 6H), 1.33 (sext, <sup>3</sup>*J* = 8 Hz, 6H), 1.14 (t, <sup>3</sup>*J* = 8 Hz, 6H), 0.88 (t, <sup>3</sup>*J* = 8 Hz, 9H). <sup>13</sup>C NMR (CDCl<sub>3</sub>, δ) 187.1 (C), 163.5 (C), 118.1 (CH), 29.0 (CH<sub>2</sub>), 27.2 (CH<sub>2</sub>), 24.1 (CH<sub>3</sub>), 13.7 (CH<sub>2</sub>), 10.2 (CH<sub>3</sub>). <sup>119</sup>Sn NMR (CDCl<sub>3</sub>, δ) −74.2. Elemental analysis calcd (%) for C<sub>18</sub>H<sub>34</sub>N<sub>2</sub>Sn: C 54.43, H 8.63, N 7.05. Found: C 54.31, H 8.66, N 7.03.

**Synthesis of 1-Bromo-4-chloro-2,6-bis(4,6-dimethyl-2-pyrimidinyl)benzene (10).** A mixture of **8** (222 mg, 0.501 mmol), **9** (421 mg, 1.06 mmol), PdCl<sub>2</sub>(PPh<sub>3</sub>)<sub>2</sub> (72 mg, 0.10 mmol), and LiCl (142 mg, 3.35 mmol) in *p*-xylene (2.5 mL) was heated under reflux for 23 h and then cooled to room temperature. The reaction mixture was filtered through Celite and the Celite was washed with AcOEt (5 mL). The filtrate was concentrated by using a rotary evaporator. The crude product was purified by column chromatography (silica gel, AcOEt: *n*-hexane = 1:1, *R<sub>f</sub>* 0.25) followed by reverse-phase HPLC (RT = 23). Compound **10** (27 mg, 0.067 mmol, 13%) was obtained as a white solid. <sup>1</sup>H NMR (CDCl<sub>3</sub>, δ) 7.60 (s, 2H), 7.04 (s, 2H), 2.55 (s, 12H). <sup>13</sup>C NMR (CDCl<sub>3</sub>, δ) 166.5 (C), 164.8 (C), 142.7 (C), 132.8 (C), 130.4 (CH), 119.0 (C), 118.4 (CH), 23.7 (CH<sub>3</sub>). HRMS (APPI, positive) calcd (*m/z*) for [M(C<sub>18</sub>H<sub>16</sub>BrClN<sub>4</sub>) + H]<sup>+</sup> 403.03196, found 403.03238. Elemental analysis calcd (%) for C<sub>6</sub>H<sub>2</sub>BrClN<sub>2</sub> with 0.25H<sub>2</sub>O: C 52.96, H 4.07, N 13.73. Found: C 52.97, H 3.90, N 13.70. Mp 160.7–161.5 °C dec.

**Synthesis of 1-Chloro-3,5-bis(4,6-dimethyl-2-pyrimidinyl)-4-(1,3,2-dioxaborolan-2-yl)benzene (11).** To a solution of **10** (245 mg, 0.607 mmol) in dry Et<sub>2</sub>O (50 mL) was added dropwise *t*-BuLi (1.55 M in *n*-pentane, 0.80 mL, 1.3 mmol) at −78 °C. After the mixture was stirred for 2 h, B(OMe)<sub>3</sub> (0.45 mL, 3.9 mmol) was added dropwise. After being stirred for 20 h, the reaction mixture was allowed to warm to room temperature. The solvent was removed by using a rotary evaporator and CH<sub>3</sub>CN (3 mL) was added to the residue. The suspension was filtered through a pad of Wakogel 50C18 and the silica gel was washed with CH<sub>3</sub>CN. The filtrate was concentrated by using a rotary evaporator. The crude product was roughly purified by reverse-phase HPLC (RT = 35). The boronic ester derivative (15 mg, 0.041 mmol, 7%) was obtained as a white solid. However, since the boronic ester derivative easily hydrolyzed to the boronic acid in the open air, further derivation was carried out. To a mixture of the hydrolysate and Na<sub>2</sub>SO<sub>4</sub> (15 mg, 0.10 mmol) were added glycol (0.39 M in dry CH<sub>2</sub>Cl<sub>2</sub>, 0.17 mL, 0.062 mmol) and dry CH<sub>2</sub>Cl<sub>2</sub> (3 mL) at room temperature. After being stirred for 72 h at room temperature, the reaction mixture was filtered through a membrane filter. To the filtrate was slowly added dry *n*-hexane (10 mL). Yellow single crystals of **11** suitable for X-ray structural analysis were obtained from the solvent mixture under a N<sub>2</sub> atmosphere. <sup>1</sup>H NMR (CD<sub>2</sub>Cl<sub>2</sub>, δ) 8.32 (s, 2H), 7.01 (s, 2H), 4.22 (s, 4H), 2.55 (s, 12H). <sup>11</sup>B NMR (CD<sub>2</sub>Cl<sub>2</sub>, −80 °C, δ) 16 (br). HRMS (ESI, positive) calcd (*m/z*) for [M (C<sub>20</sub>H<sub>20</sub>BClN<sub>4</sub>O<sub>2</sub>) + H]<sup>+</sup> 395.14406, found 395.14399. Mp 273.0–274.0 °C dec.

**X-ray Crystal Structural Analyses.** Crystals suitable for X-ray structure determination were mounted on a CCD diffractometer and irradiated with graphite monochromated Mo Kα radiation (λ = 0.71073 Å) at 173 K for data collection. The structure was solved by a direct method using the SIR-97 program.<sup>23</sup> Refinement on *F*<sup>2</sup> was carried out using full-matrix least-squares with the SHELX-97 program.<sup>24</sup> All non-hydrogen atoms were refined by using anisotropic thermal parameters. Selected structural parameters are summarized in Table 1. Crystallographic data have been deposited with the Cambridge Crystallographic Data Centre; deposition nos. CCDC-804980 and 804981 for compounds **8** and **11**, respectively. Copies of the data can be obtained free of charge via <http://www.ccdc.cam.ac.uk/conts/retrieving.html> (or from the Cambridge

Crystallographic Data Centre, 12 Union Road, Cambridge CB2 1EZ, UK; fax +44 1223 336033; e-mail deposit@ccdc.cam.ac.uk).

**Theoretical Calculations.** The MO and DFT calculations were performed with the Gaussian 09 program package.<sup>19</sup> The final geometry optimizations were performed with DFT/B3PW91,<sup>25</sup> with the 6-31G-(d) basis set for all atoms. No symmetry constraints were imposed during these optimizations.

The energy diagram for **11** with restricted rotation of the pyrimidine ring (Figure 6) was obtained by plotting the energies of optimized structures with dihedral angles varying from 0° to 90° in 5° increments. Structures of **12**, **13**, and **14** were found by optimization of initial structures with pyrimidyl–phenyl with two dihedral angles of 0°, 0° (12-DFT), 15°, 15° (13-DFT), and 90°, 0° (14-DFT), respectively.

## ■ ASSOCIATED CONTENT

**S Supporting Information.** Spectroscopic and crystallographic data for new compounds, and atomic coordinates for the calculated structures and CIF files for **8** and **11**. This material is available free of charge via the Internet at <http://pubs.acs.org>.

## ■ AUTHOR INFORMATION

### Corresponding Author

yyama@sci.hiroshima-u.ac.jp

## ■ ACKNOWLEDGMENT

This work was supported by Grants-in-Aid for Scientific Research (Nos. 17350021 and 21350029) from the Ministry of Education, Culture, Sports, Science and Technology of the Japanese Government. The authors thank Mr. Hitoshi Fujitaka and Dr. Daisuke Kajiya of the Natural Science Center for Basic Research and Development (N-BARD), Hiroshima University for VT-NMR (600 MHz) measurements and HRMS measurements, respectively. The computations were performed using the Research Center for Computational Science, Okazaki, Japan and Information Media Center, Hiroshima University.

## ■ REFERENCES

- (1) Akiba, K.-y. *Chemistry of Hypervalent Compounds*; Wiley-VCH: New York, 1999.
- (2) For theoretical calculations on hypervalent nitrogen see: (a) Ewig, C. S.; Van Wazer, J. R. *J. Am. Chem. Soc.* **1989**, *111*, 4172–4178. (b) Michels, H. H.; Montgomery, J. A., Jr. *J. Chem. Phys.* **1990**, *93*, 1805–1813. (c) Bettinger, H. F.; Schleyer, P. v. R.; Schaefer, H. F., III. *J. Am. Chem. Soc.* **1998**, *120*, 11439–11448. (d) Ponec, R.; Roithova, J. *Theor. Chem. Acc.* **2001**, *105*, 383–392.
- (3) For theoretical calculations on hypervalent carbon see: (a) Gutsev, G. L. *Chem. Phys.* **1992**, *166*, 57–68. (b) Pierrefixe, S. C. A. H.; Poater, J.; Im, C.; Bickelhaupt, F. M. *Chem.—Eur. J.* **2008**, *14*, 6901–6911. (c) Pierrefixe, S. C. A. H.; van Stralen, S. J. M.; van Stralen, J. N. P.; Fonseca Guerra, C.; Bickelhaupt, F. M. *Angew. Chem., Int. Ed.* **2009**, *48*, 6469–6471. (d) Kikuchi, Y.; Ishii, M.; Akiba, K.-y.; Nakai, H. *Chem. Phys. Lett.* **2008**, *460*, 37–41. (e) Atsumi, T.; Abe, T.; Akiba, K.-y.; Nakai, H. *Bull. Chem. Soc. Jpn.* **2010**, *83*, 892–899.
- (4) (a) Forbus, T. R., Jr.; Martin, J. C. *J. Am. Chem. Soc.* **1979**, *101*, 5057–5059. (b) Martin, J. C. *Science* **1983**, *221*, 509–514. (c) Lee, D. Y.; Martin, J. C. *J. Am. Chem. Soc.* **1984**, *106*, 5745–5746. (d) Forbus, T. R., Jr.; Martin, J. C. *Heteroatom Chem.* **1993**, *4*, 129–136. (e) Hojo, M.; Ichi, T.; Shibato, K. *J. Org. Chem.* **1985**, *50*, 1478–1482.
- (5) (a) Akiba, K.-y.; Yamashita, M.; Yamamoto, Y.; Nagase, S. *J. Am. Chem. Soc.* **1999**, *121*, 10644–10645. (b) Yamashita, M.; Yamamoto, Y.; Akiba, K.-y.; Nagase, S. *Angew. Chem., Int. Ed.* **2000**, *39*, 4055–4058.

(c) Yamashita, M.; Yamamoto, Y.; Akiba, K.-y.; Hashizume, D.; Iwasaki, F.; Takagi, N.; Nagase, S. *J. Am. Chem. Soc.* **2005**, *127*, 4354–4371.

(6) Emsley, J. *The Elements*, 3rd ed.; Oxford University Press: Oxford, UK, 1998.

(7) Yamaguchi, T.; Yamamoto, Y.; Kinoshita, D.; Akiba, K.-y.; Zhang, Y.; Reed, C. A.; Hashizume, D.; Iwasaki, F. *J. Am. Chem. Soc.* **2008**, *130*, 6894–6895.

(8) Yano, T.; Yamaguchi, T.; Yamamoto, Y. *Chem. Lett.* **2009**, *38*, 794–795.

(9) (a) Akiba, K.-y.; Moriyama, Y.; Mizozoe, M.; Inohara, H.; Nishii, T.; Yamamoto, Y.; Minoura, M.; Hashizume, D.; Iwasaki, F.; Takagi, N.; Ishimura, K.; Nagase, S. *J. Am. Chem. Soc.* **2005**, *127*, 5893–5901. (b) Nakatsuji, J.-y.; Moriyama, Y.; Matsukawa, S.; Yamamoto, Y.; Akiba, K.-y. *Main Group Chem.* **2006**, *5*, 277–285.

(10) Nakatsuji, J.-y.; Yamamoto, Y. *Bull. Chem. Soc. Jpn.* **2010**, *83*, 767–776.

(11) (a) Yamashita, M.; Watanabe, K.; Yamamoto, Y.; Akiba, K.-y. *Chem. Lett.* **2001**, 1104–1105. (b) Yamashita, M.; Kamura, K.; Yamamoto, Y.; Akiba, K.-y. *Chem.—Eur. J.* **2002**, *8*, 2976–2979. (c) Yamashita, M.; Mita, Y.; Yamamoto, Y.; Akiba, K.-y. *Chem.—Eur. J.* **2003**, *8*, 3655–3659. (d) Yamaguchi, T.; Yamamoto, Y. *Chem. Lett.* **2007**, *36*, 1438–1439.

(12) (a) Toyota, S.; Futawaka, T.; Ikeda, H.; Ōki, M. *J. Chem. Soc., Chem. Commun.* **1995**, 2499–2500. (b) Toyota, S.; Futawaka, T.; Asakura, M.; Ikeda, H.; Ōki, M. *Organometallics* **1998**, *17*, 4155–4163.

(13) Toyota, S.; Uemitsu, N.; Ōki, M. *Heteroatom Chem.* **2004**, *15*, 241–245.

(14) (a) Akiba, K.-y.; Ohsugi, M.; Iwasaki, H.; Ohkata, K. *J. Am. Chem. Soc.* **1988**, *110*, 5576–5578. (b) Ohkata, K.; Ohsugi, M.; Yamamoto, K.; Ohsawa, M.; Akiba, K. *J. Am. Chem. Soc.* **1996**, *118*, 6355–6369. (c) Yamauchi, Y.; Akiba, K.-y.; Nakai, H. *Chem. Lett.* **2007**, *36*, 1120–1121. (d) Atsumi, T.; Abe, T.; Akiba, K.-y.; Nakai, H. *Bull. Chem. Soc. Jpn.* **2010**, *83*, S20–S29.

(15) Hirano, Y.; Saiki, Y.; Taji, H.; Matsukawa, S.; Yamamoto, Y. *Heterocycles* **2008**, *76*, 1585–1592.

(16) Charrier, N.; Demont, E.; Dunsdon, R.; Maile, G.; Naylor, A.; O'Brien, A.; Redshaw, S.; Theobald, P.; Vesey, D.; Walter, D. *Synthesis* **2006**, 3467–3477.

(17) Sun, C.; Lin, X.; Weinreb, S. M. *J. Org. Chem.* **2006**, *71*, 3159–3166.

(18) Wilkinson, A. J.; Pushmann, H.; Howard, J. A. K.; Foster, C. E.; Williams, J. A. G. *Inorg. Chem.* **2006**, *45*, 8685–8699.

(19) Frisch, M. J.; et al. *Gaussian 09*, Revision A.02; Gaussian, Inc., Wallingford, CT, 2009.

(20) Hydrogen bonding between a pyrimidine nitrogen and an ortho proton of the phenyl group can also be envisioned, thus giving rise to two more interactions in the coplanar conformation of **13**. However, since this hydrogen bonding includes interaction involving a C–H bond, the H–N distance is long (2.32 Å), and the orientation of the C–H bond is essentially orthogonal to the direction of the supposed sp<sup>2</sup> lone pair of the nitrogen atom of the pyrimidine ring; this contribution should be insignificant compared with the stabilization gained by aryl–aryl  $\pi$ -conjugation.

(21) Vlád, G.; Horváth, I. T. *J. Org. Chem.* **2002**, *67*, 6550–6552.

(22) Dains, F. B.; Vaughan, T. H.; Janney, W. M. *J. Am. Chem. Soc.* **1918**, *40*, 930–936.

(23) Altomare, A.; Burla, M. C.; Camalli, M.; Cascarano, G. L.; Giacovazzo, C.; Guagliardi, A.; Moliterni, A. G. G.; Polidori, G.; Spagna, R. *J. Appl. Crystallogr.* **1999**, *32*, 115–119.

(24) Sheldrick, G. M. *SHELX-97*, Program for the Refinement of Crystal Structures; University of Gottingen: Gottingen, Germany, 1997.

(25) (a) Becke, A. D. *Phys. Rev. A* **1988**, *38*, 3098–3100. (b) Becke, A. D. *J. Chem. Phys.* **1993**, *98*, 5648–5652. (c) Perdew, J. P.; Wang, Y. *Phys. Rev. B* **1992**, *45*, 13244–13249.